

Determination of adsorption entropies on solid surfaces by reversed-flow gas chromatography

A.V. Dremetsika^a, P.A. Siskos^a, N.A. Katsanos^{b,*}

^a Environmental Analysis Group, Laboratory of Analytical Chemistry, Department of Chemistry, University of Athens, Panepistimioupoli, 15771 Zografos, Athens, Greece

^b Physical Chemistry Laboratory, University of Patras, 26504 Patras, Greece

Available online 5 July 2007

Abstract

The reversed-flow gas chromatography (RF-GC) method has been applied to measure the time separation of adsorption entropies and their probability density functions, when acetic and formic acid vapors, responsible for artifacts degradation inside museums, are adsorbed on various heterogeneous surfaces. The solid materials studied were Penteli marble and solid metals (lead, copper and iron), which are commonly used for the construction of the artifacts. Physicochemical measurements were performed at various temperatures in the range 353–473 K, the surface coverage θ being also calculated over time. A new mathematical model, based on well known equations was used in order to extract the above quantities. © 2007 Elsevier B.V. All rights reserved.

Keywords: Adsorption entropy; Inverse gas chromatography; Heterogeneous surfaces

1. Introduction

An important part of the protection and restoration of the environment consists of protecting and restoring solid surfaces, mainly from damage caused by air pollutants on art pieces and other objects of cultural value. It seems that old inverse gas chromatography cannot distinguish various adsorption sites, as regards adsorption energy and entropy. Contrasted to that, time-resolved inverse gas chromatography can make some noticeable distinctions of adsorption entropy distribution functions against time of measurement. It is thus interesting to measure adsorption entropies, particularly when volatile organic acids, like acetic and formic acids are involved.

These acids are the most common organic acids that accumulate in big concentrations in the interior atmosphere of display cases and cabinets of museums, where many artifacts and objects of artistic value are usually exposed [1]. They are usually come from many types of wood used for the construction of the display cases and mounting materials such as paints and varnishes, as well as from various things placed inside the cases [2]. It has also

been detected that these two small-chain organic compounds are responsible for the degradation and chemical damage of the above objects, when these are constructed of materials such as marble and metals [3–5].

Some analytical measurements of the two acids inside European museums have already been performed [6,7]. Although estimation of the concentration levels of pollutants seems necessary for risk assessment, only measurements of various physicochemical parameters over time give information on the real mechanism of the material's damage. Inverse gas chromatography has made several steps towards this direction [8].

In the present work, reversed-flow gas chromatography (RF-GC) [9], has been applied to measure the time separation of adsorption entropies and their probability density functions, when acetic and formic acid vapors are adsorbed on the heterogeneous surfaces of Penteli marble and metals, like lead, copper and iron. A new mathematical model was used in order to extract the above quantities, while the calculations were carried out by a simple PC program.

2. Theory

The time distribution of adsorption entropy of gases on heterogeneous surfaces [10] started in 1978 by Katsanos et al. [11] who have determined experimentally both the differential

* Corresponding author at: Department of Chemistry, University of Patras, 26504 Patras, Greece. Tel.: +30 2610 321934; fax: +30 2610 997144.

E-mail addresses: dremetsika@chem.uoa.gr (A.V. Dremetsika), siskos@chem.uoa.gr (N.A. Katsanos).

enthalpy ΔH_{ads} and the differential entropy of adsorption ΔS_{ads} based on the equation:

$$\ln V_N = \ln(RTn_s) + \frac{S_{\text{ads}}}{R} - \frac{H_{\text{ads}}}{R} \frac{1}{T} \quad (1)$$

where V_N is the net retention volume of gas chromatography, and n_s the total amount of the substance in the adsorbed state. The method was based on the variation of V_N with temperature.

Later Knox and Dadyburjor [12] developed the bounds for acceptable values of adsorption entropy. In 1993, Lopez-Garzon et al. [13] used simple inverse gas chromatography to calculate standard free energy, enthalpy and entropy of adsorption of n-alkanes using the equation $\Delta S = (\Delta H - \Delta G)/T$. Keeping in mind that $\Delta G = -RT \ln K_{\text{exp}}$, one finds by substituting $-RT \ln K_{\text{exp}}$ for ΔG in the first relation and rearrangement

$$\ln K_{\text{exp}} = \frac{S}{R} - \frac{H}{RT} \quad (2)$$

More recently Bakaev and co-workers [14,15,16,17] used inverse gas chromatography to study the entropy distribution of adsorption sites on heterogeneous glass fiber surface. The classical Eq. (2) has been derived again [16] in the form:

$$K'_H = \exp\left(\frac{S_i}{R}\right) \exp\left(-\frac{U_i}{RT}\right) \quad (3)$$

where K'_H is the Henry constant, and ΔU_i and ΔS_i are the changes of the energy and the entropy, respectively, for a mol of molecules adsorbed on i -sites and the ideal gas state.

The necessary mathematical model for calculating the adsorption entropy as a time-resolved quantity, can be based on Adsorption Entropies as described by Adamson and Gast [18]. Their relevant equation for localized adsorption with configurational entropy as the only contribution is:

$$\Delta \bar{S}^{\circ}_{\text{ads local}} = -R \ln\left(\frac{\theta}{1-\theta}\right) - \bar{S}_{\text{trans}}^{0,g} \quad (4)$$

$$f(\Delta S; t) = \frac{\partial c_{\text{max}}^* / \partial t}{\partial(\Delta S) / \partial t} = \frac{\partial c_{\text{max}}^*}{\partial(\Delta S)} \quad (5)$$

where $\bar{S}_{\text{trans}}^{0,g}$ is the translational entropy, θ is the local adsorption isotherm, which can be calculated as described by the Jovanovich isotherm [10]:

$$\theta(p, T, \varepsilon) = 1 - \exp(-Kp) \quad (6)$$

and c_{max}^* is the maximum local monolayer capacity of the adsorbate.

The probability density function for the adsorption entropy, defined from Eq. (5), can be considered as a time function, t being a structural parameter of time and not a random variable. The function $\varphi(\Delta S; t)$:

$$\varphi(\Delta S; t) = \theta f \frac{(\Delta S; t)}{c_{\text{max}}^*} \quad (7)$$

seems a better choice for the true entropy distribution function, being an explicit function of the random variable ΔS and the structural parameter t , as found in previous work [19] for the

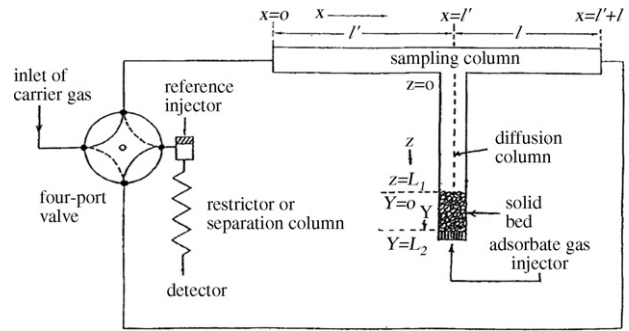


Fig. 1. Experimental set-up for RF-GC method.

analogous probability density function of the adsorption energy, ε :

$$\varphi(\varepsilon; t) = \theta \frac{f(\varepsilon)}{c_{\text{max}}^*} \quad (8)$$

3. Materials and methods

3.1. Experimental arrangement

The experimental set-up has been described several times before [9,20] and it is presented in Fig. 1 for convenience.

The chromatograph was a Perkin Elmer Sigma 3B model equipped with a flame ionization detector (FID) and the carrier gas was nitrogen. The section L_1 of the diffusion column was of length 58 cm and remained empty of any solid material. The section L_1 (8.0–9.0 cm) contained 0.6–2.8 g of each solid studied, having particle sizes 20–30 mesh. The sampling column $l' + l$ (73.0 + 75.0 cm) was made from a stainless steel chromatographic tube of 4 mm i.d. A restrictor was used in front of the detector to protect the flame.

3.2. Procedure

The procedure consists of repeatedly reversing for 5 s the direction of the carrier gas flow for 5 s by means of the four-port gas sampling valve. Following each flow reversal, an extra narrow “sample peak” [9,10] appears in the recorder (Fig. 2). Measurements were performed at various temperatures in the range 353–473 K. The series of the sample peaks recorded obey

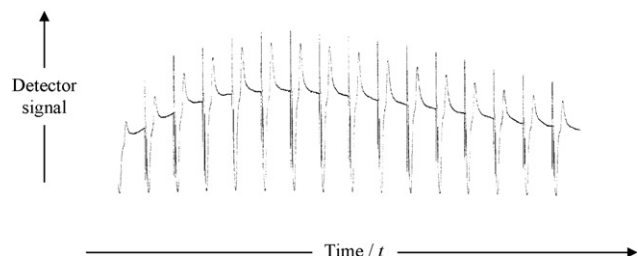


Fig. 2. Sample peaks obtained after repeated flow reversals of the carrier gas for 5 s.

Table 1

Typical results of local adsorption isotherms (θ), local adsorption entropies ($-\Delta\bar{S}^{\circ}_{\text{ads}}$) and entropy distribution functions [$\varphi(\Delta S; t)$] for acetic and formic acid vapors on marble, lead, copper and iron at 353 K in specific times

CH ₃ COOH				HCOOH			
t (min)	θ (dimensionless)	$-\Delta\bar{S}^{\circ}_{\text{ads}}$ (J/mol K) local	$100\varphi(\Delta S; t)$ (mol K/J)	t (min)	θ (dimensionless)	$-\Delta\bar{S}^{\circ}_{\text{ads}}$ (J/mol K) local	$100\varphi(\Delta S; t)$ (mol K/J)
Marble							
2	0.0001	84.9	0.003	2	0.0011	103.6	0.039
98	1.0000	895.2	0.000	12	0.5101	160.4	2.974
108	0.5432	164.8	2.985	16	1.0000	891.9	0.000
142	0.8682	179.0	1.376	26	0.1188	143.4	1.202
190	0.2057	152.1	1.965	50	0.0470	135.0	0.379
Lead							
2	0.6634	169.0	25.409	2	0.0368	132.9	11.581
40	1.0000	895.2	0.000	116	1.0000	891.9	0.000
96	0.4377	161.3	2.888	124	0.3553	155.1	2.755
126	0.9389	186.1	53.564	184	0.9996	224.3	0.004
230	0.4549	161.1	1.948	210	1.0000	891.9	0.000
Copper							
2	0.0000	67.6	0.001	2	0.0336	132.1	8.514
90	0.0096	124.9	0.115	88	0.2552	151.2	2.318
140	0.1150	146.4	1.224	96	0.8075	172.0	1.870
150	1.0000	895.2	0.000	112	0.5901	163.1	2.909
170	0.6404	168.2	2.770	170	1.0000	891.9	0.000
Iron							
2	0.0212	131.5	2.661	2	0.0159	125.8	2.571
50	1.0000	895.2	0.000	76	0.5964	163.3	2.882
70	0.7490	172.5	2.232	92	1.0000	891.9	0.000
126	0.9999	237.5	0.068	116	0.1075	142.5	1.154
190	0.3023	156.4	2.275	170	0.9938	202.2	0.024

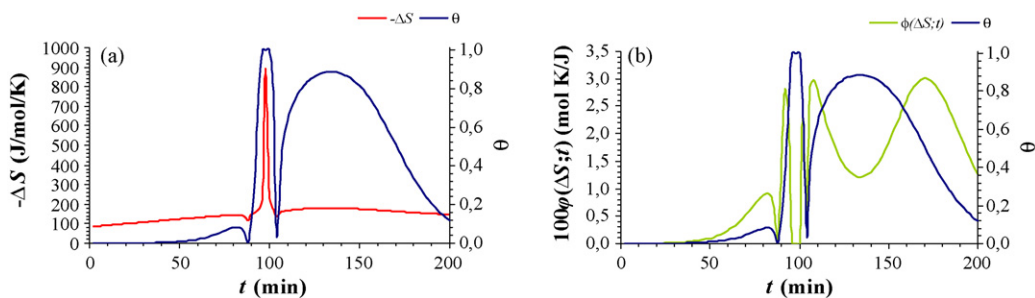


Fig. 3. Time distribution of (a) local adsorption entropy (left ordinate) and (b) entropy distribution function (left ordinate) together with the time distribution of local adsorption isotherm (right ordinate) for the system *marble–acetic acid* at 353 K.

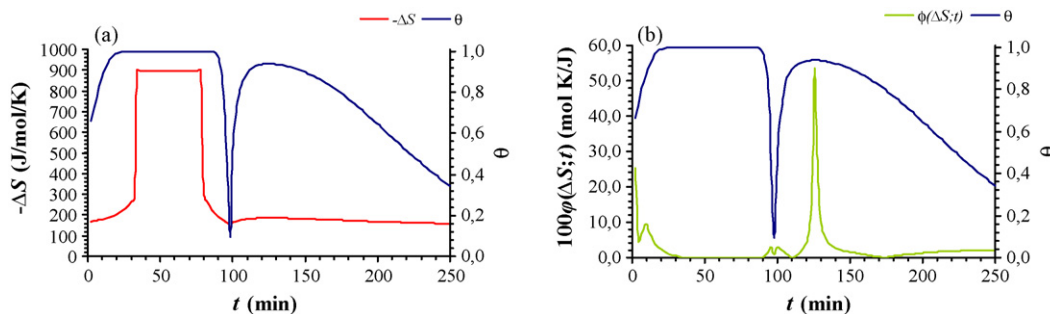


Fig. 4. Time distribution of (a) local adsorption entropy (left ordinate) and (b) entropy distribution function (left ordinate) together with the time distribution of local adsorption isotherm (right ordinate), for the system *lead–acetic acid* at 353 K.

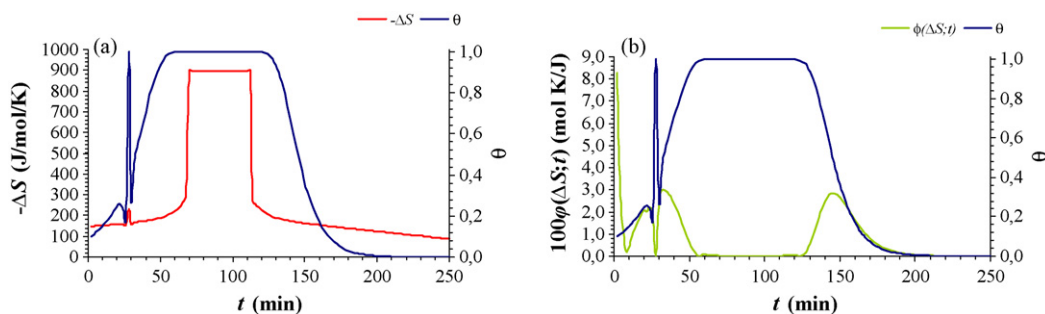


Fig. 5. Time distribution of (a) local adsorption entropy (left ordinate) and (b) entropy distribution function (left ordinate) together with the time distribution of local adsorption isotherm (right ordinate) for the system *copper–acetic acid* at 353 K.

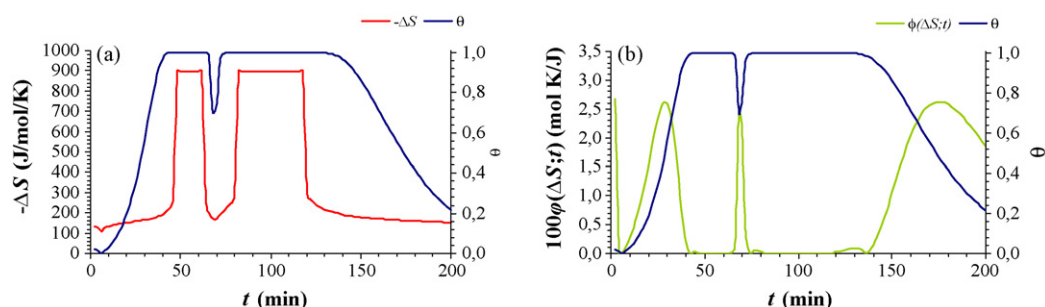


Fig. 6. Time distribution of (a) local adsorption entropy (left ordinate) and (b) entropy distribution function (left ordinate) together with the time distribution of local adsorption isotherm (right ordinate) for the system *iron–acetic acid* at 353 K.

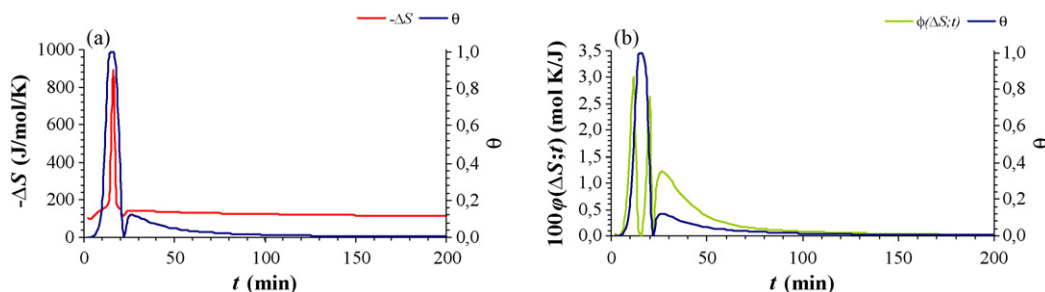


Fig. 7. Time distribution of (a) local adsorption entropy (left ordinate) and (b) entropy distribution function (left ordinate) together with the time distribution of local adsorption isotherm (right ordinate) for the system *marble–formic acid* at 353 K.

fairly accurately an equation of the form:

$$H^{1/M} = \sum_{i=1}^3 A_i \exp(B_i t) \quad (9)$$

where H is the net-height of each sample peak, M is the response factor of the detector (1 for a flame ionization detector), and A_i , B_i are functions of the physicochemical quantities pertaining to the various physicochemical phenomena occurring in the region of the solid bed. The experimental values of A_i and B_i ($i = 1-3$)

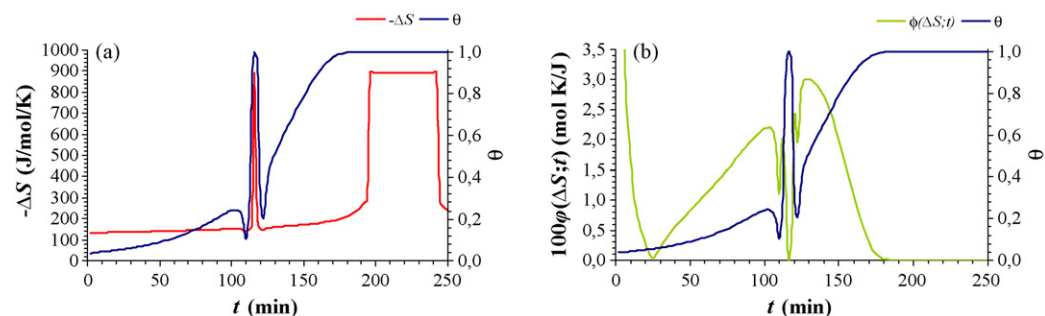


Fig. 8. Time distribution of (a) local adsorption entropy (left ordinate) and (b) entropy distribution function (left ordinate) together with the time distribution of local adsorption isotherm (right ordinate) for the system *lead–formic acid* at 353 K.

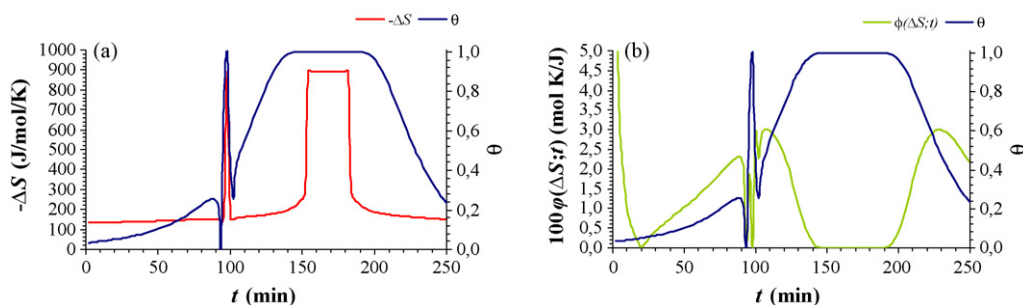


Fig. 9. Time distribution of (a) local adsorption entropy (left ordinate) and (b) entropy distribution function (left ordinate) together with the time distribution of local adsorption isotherm (right ordinate) for the system *copper–formic acid* at 353 K.

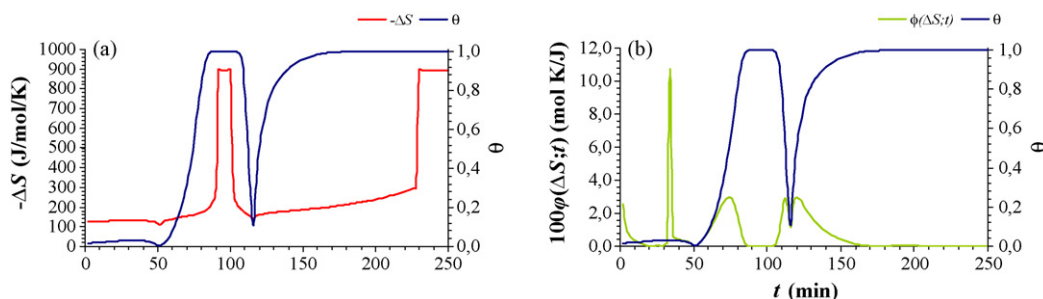


Fig. 10. Time distribution of (a) local adsorption entropy (left ordinate) and (b) entropy distribution function (left ordinate) together with the time distribution of local adsorption isotherm (right ordinate) for the system *iron–formic acid* at 353 K.

are found from a non-linear least-squares regression analysis, included in a simple PC program. By entering the values of some other quantities needed (temperature, diffusion coefficient D_z , molar mass, geometrical characteristics of the cell, etc.), one obtains the final results required, like $\Delta\bar{s}_{\text{ads}}^{\circ}$ (Eq. (4)),

local

$\theta(p, T, \varepsilon)$ Eq. (6) and $\varphi(\Delta S; t)$ (Eq. (7)).

4. Results and discussion

Some representative results of calculation of adsorption entropies and their probability density functions, as well as the local adsorption isotherm (surface coverage θ), for specific times and for all gas–solid systems studied at temperature 353 K are shown in Table 1.

By plotting time distribution of adsorption entropy and its probability density function over time in the same diagram together with local adsorption isotherm θ also as a function of time, certain conclusions can be drawn. These time distributions are presented for each gas–solid system in Figs. 3–10.

5. Conclusion

From the results obtained, it is obvious that for all gas–solid systems adsorption entropy increases with surface coverage θ and generally follows its ups and downs. In addition one can also conclude that, when surface coverage reaches the value 1.000, the difference of the adsorption entropy stays constant, i.e. adsorption entropy does not change during this time period. This can be easily explained, since the system disorder is expressed

via adsorption entropy, which takes its minimum value when the studied adsorption phenomenon stops developing. On the other hand, the distribution function $\varphi(\Delta S; t)$ changes irregularly but not much as θ increases. It is also obvious from Table 1 and the Figs. 2–9 that it reaches zero when local adsorption isotherm reaches the value 1.

References

- [1] P. Brimblecombe, The composition of museum atmospheres: review, *Atmos. Environ.* B 24 (1) (1990) 1–8.
- [2] C. Grzywacz, N. Tennent, The threat of organic carbonyl pollutants to museum collections, effects of the environment on indoor cultural property, in: European Commission Research Workshop, Wurzburg, Germany, 1995.
- [3] N. Tennent, B.G. Cooksey, D. Littlejohn, B.J. Ottaway, S.E. Tarling, M. Vickers, Unusual corrosion and efflorescence products on bronze and iron antiquities stored in wooden cabinets, in: Conservation Science in the U.K.: Preprints of the Meeting held in Glasgow, James & James, 1993.
- [4] J. Tétreault, E. Cano, M. Van Bommel, D. Scott, M. Dennis, M.G. Barthés-Labrousse, L. Minel, L. Robbiola, Corrosion of copper and lead by formaldehyde, formic and acetic acid vapours, *Stud. Conserv.* 48 (4) (2004) 237–250.
- [5] L.T. Gibson, B.G. Cooksey, D. Littlejohn, N.H. Tennent, Investigation of the composition of a unique efflorescence on calcareous museum artifacts, *Anal. Chim. Acta* 337 (1997) 253–264.
- [6] A.V. Dremetsika, P.A. Siskos, E.B. Bakeas, Determination of formic and acetic acid in the interior atmosphere of display cases and cabinets in museums of Athens by reverse phase high performance liquid chromatography, *Indoor Built Environ.* 14 (1) (2005) 51–58.
- [7] M. Ryhl-Svendsen, J. Glastrup, Acetic acid and formic acid concentrations in the museum environment measured by SPME-GC/MS, *Atmos. Environ.* 36 (2002) 3909–3916.
- [8] N.A. Katsanos, Physicochemical measurements by the reversed-flow version of inverse gas chromatography: review, *J. Chromatogr. A* 969 (2002) 3–8.

- [9] N.A. Katsanos, G. Karaiskakis, *Time Resolved Inverse Gas Chromatography and its Applications*, HNB Publishing, New York, 2004.
- [10] N.A. Katsanos, G. Kapolos, D. Gavril, N. Bakaoukas, V. Loukopoulos, A. Koliadima, G. Karaiskakis, Time distribution of adsorption entropy of gases on heterogeneous surfaces by reversed-flow gas chromatography, *J. Chromatogr. A* 1127 (2006) 221–227.
- [11] N.A. Katsanos, A. Lycourghiotis, A. Tsiatsios, Thermodynamics of adsorption based on gas–solid chromatography, *J. Chem. Soc. Farad. Trans. 1* (74) (1978) 575–582.
- [12] D. Knox, D.B. Dadyburjor, Bounds for acceptable values of adsorption entropy, *Chem. Eng. Commun.* 11 (1981) 99–112.
- [13] F.J. Lopez-Garzon, M. Pyda, M. Domingo-Garcia, Studies of the surface properties of active carbons by inverse gas chromatography at infinite dilution, *Langmuir* 9 (1993) 531–536.
- [14] T.I. Bakaeva, V.A. Bakaev, C.G. Pantano, Adsorption of CO₂ on glass fibers, *Langmuir* 9 (2000) 531–536.
- [15] T.I. Bakaeva, C.G. Pantano, C.T. Loupe, V.A. Bakaev, Heterogeneity of the glass fiber surface from inverse gas chromatography, *J. Phys. Chem. B* 104 (2000) 8518–8526.
- [16] T.I. Bakaeva, V.A. Bakaev, C.G. Pantano, Surface heterogeneity and surface area from linear inverse gas chromatography—application to glass fibers, *J. Chromatogr. A* 969 (2002) 153–165.
- [17] T.I. Bakaeva, V.A. Bakaev, C.G. Pantano, A study of glass surface heterogeneity and silylation by inverse gas chromatography, *J. Phys. Chem. B* 106 (2002) 12231–12238.
- [18] A.W. Adamson, A.P. Gast, *Physical Chemistry of Surfaces*, Wiley, 1997, pp. 612–613.
- [19] N.A. Katsanos, E. Iliopoulou, V. Plagianakos, H. Mangou, Interrelations between adsorption energies and local isotherms, local monolayer capacities and energy distribution functions as determined for heterogeneous surfaces by inverse gas chromatography, *J. Colloid Interf. Sci.* 239 (2001) 10–19.
- [20] N.A. Katsanos, E. Arvanitopoulou, F. Roubani-Kalantzopoulou, A. Kalantzopoulos, Time distribution of adsorption energies, local monolayer capacities and local isotherms on heterogeneous surfaces by inverse gas chromatography, *J. Phys. Chem. B* 103 (1999) 1152–1157.